Superconducting, energy variable heavy ion linac with constant β, multicell cavities of CH-type

S. Minaev,[1,*] U. Ratzinger,[1] H. Podlech,[1] M. Busch,[1] and W. Barth[2]

[1]*Institute for Applied Physics (IAP), University of Frankfurt, 60438 Frankfurt, Germany*

[2]*GSI Darmstadt, Planckstraße 1, 64291 Darmstadt, Germnay*

(Received 19 June 2009; published 2 December 2009)

An energy variable ion linac consisting of multigap, constant-β cavities was developed. The effect of phase sliding, unavoidable in any constant-β section, is leading to a coherent rf phase motion, which fits well to the H-type structures with their long π-mode sections and separated lenses. The exact periodicity of the cell lengths within each cavity results in technical advantages, such as higher calculation accuracy when only one single period can be simulated, simpler manufacturing, and tuning. This is most important in the case of superconducting cavities. By using this concept, an improved design for a 217 MHz cw superconducting heavy ion linac with energy variation has been worked out. The small output energy spread of ± 3 AkeV is provided over the whole range of energy variation from 3.5 to 7.3 AMeV. These capabilities would allow for a competitive research in the field of radiochemistry and for a production of super heavy elements (SHE), especially. A first 19-cell cavity of that type was designed, built, and rf tested successfully at the Institute for Applied Physics (IAP) Frankfurt. A 325.224 MHz, seven-cell cavity with constant $\beta = 0.16$ is under development and will be operated in a frequency controlled mode. It will be equipped with a power coupler and beam tests with Unilac beams at GSI are foreseen.

DOI: 10.1103/PhysRevSTAB.12.120101 PACS numbers: 29.20.Ej, 85.25.−j

I. INTRODUCTION

This paper is investigating the design and possible technical parameters of a cw operated linac to perform experiments with heavy ions at the Coulomb barrier.

The linac design described in this paper investigates the potential of cavities with gap numbers from 10 to 20 and with cold focusing elements located in the intertank sections. One cryostat might house several cavities and lenses. While cavity lengths will range up to around 1 m, the cylindrical cryostats might be about 5 m in length, typically. At a given frequency, H-type cavities are very attractive because of their small transverse dimensions [1]. A 19-cell 360 MHz prototype shown at Fig. 1 was successfully developed and operated at IAP Frankfurt [2]. In close cooperation with manufacturer Research Instruments (RI) GmbH, Bergisch Gladbach, Germany, further progress in the development of that accelerator technique is expected.

An equidistant multigap structure (EQUUS) in combination with external focusing lenses has been found and studied in detail. The study results are presented in this paper. This concept allows negative rf phases at the entrance and exit regions and acceleration around the crest of the wave along the middle part. This is also the strategy followed in KONUS (combined zero degree sections) designs [1,3,4], allowing a maximum in accelerating voltage between two neighboring focusing lenses. At the same time, EQUUS can be preferable from the viewpoint of manufacturing and rf tuning when applicable. This is of even higher importance for superconducting structures. Unlike a conventional accelerating cavity with the individual sizes of every tube and gap, the equidistant structure may consist of identical cells, each including one tube and one gap. If a flat rf voltage distribution along the cavity is expected, operating frequency and shunt impedance may be found by the electrodynamics simulations of one single cell. Calculation accuracy becomes much higher in this case and allows avoiding the ''cold'' rf model. The general features of this structure as well as the results of the beam dynamics simulations are presented below.

So far, superconducting energy variable linacs are composed by two or three gap cavities of the spiral, quarter wave, half wave, or spoke type, respectively [5–8]. This gives a high flexibility in beam energies and charge-to-mass ratios of the beam particles—just by altering rf phase relations between cavities and matching the voltage amplitudes. Disadvantages of this concept are the relatively long drifts between those short accelerating sections and the high total number of cavities with all their couplers, tuners, controls, and rf power amplifiers. In many cases, the focusing elements are operated at room temperature. This causes an additional effort in a high number of separated cryostats accompanied by many cold-warm transitions along the beam line.

Unlike conventional accelerating cavities with the individual sizes of every tube and gap, the equidistant structure may consist of identical cells, each including one tube and one gap. If the flat rf voltage distribution along the cavity is expected, operating frequency and shunt impedance may be found by the electrodynamics simulation of one single cell. Calculation accuracy becomes much higher in this case and allows avoiding the cold rf model.

*Permanent address: Institute for Theoretical and Experimental Physics (ITEP), 11728 B. Cheremushkinskaya, 25 Moscow, Russia.

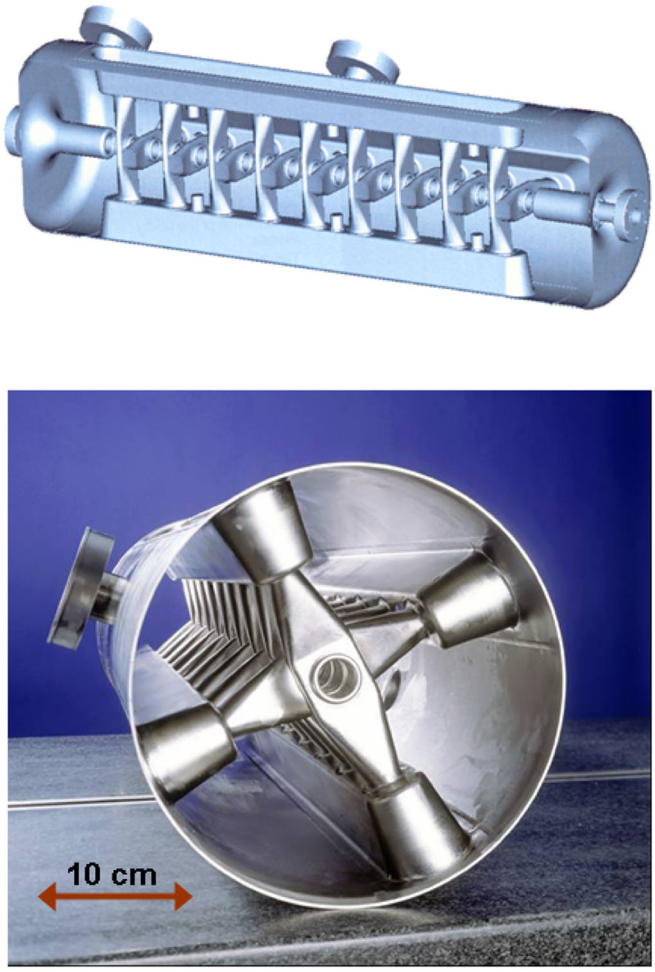

FIG. 1. (Color) Technical layout of the CH-prototype cavity (top), view into the superconducting CH cavity (bottom).

II. THE EQUUS CONCEPT

When an ion linac will become an industrial product, manufacturing technology must be adapted to the production standards, avoiding sophisticated units and minimizing individual tuning procedures. It is especially important for superconducting structures, where tuning possibilities after manufacturing are limited to relatively small ranges.

A common way of the accelerating structure design starts from the beam dynamics simulations assuming some preliminary gap voltage distribution. The desirable longitudinal motion has to be realized at this stage in terms of particle phases related to the assumed accelerating field. Since the cell length of traditional synchronous phase structures follows the particle velocity, an exactly periodic structure is not possible in the case of acceleration or deceleration. Moreover, the gap field distribution depends on the channel geometry and vice versa. For this reason, a successive approximation method for the structure combining electrodynamics and beam dynamics simulations is applied.

The well-known Alvarez and Wideroe drift tube linacs (DTL) with tube-integrated focusing lenses use the constant or slightly varied synchronous phase around -30 degrees, providing longitudinal focusing at each accelerating gap; the periodic lengths are steadily increased in these structures according to the particle velocity. Being simple and reliable for longitudinal beam stability, the bunching mechanism with a constant negative synchronous phase needs an adequate transversely focusing system in order to compensate the strong defocusing effect from the bunching field component. This is the reason why every drift tube in the Alvarez linac is housing a quadrupole lens as well as every or every second tube in Wideroe-type structures. Since the capacitive load of the drift tube structure is strongly influenced by the tube size, large tube-integrated lenses cost additional rf power and lead to lower sparking limits [9].

Unlike traditional DTLs, interdigital H-type (IH) and CH structures use the efficient multigap accelerating sections in combination with separated focusing lenses. Following a special type of beam dynamics named KONUS, particles are rebunched at the entrance of every section, then the bunch is shifted to the crest of the accelerating field (zero degree phase) and gradually slides to the negative rf phase again. This kind of longitudinal motion allows maintaining both transverse and longitudinal stability of the bunch along extended drift tube sections which contains no transversally focusing elements. Although some additional emittance growth may be expected compared to the traditional focusing lattice, high accelerating rate and rf power efficiency provided by H-type cavities with KONUS make it preferable in many practical cases.

The proposed EQUUS concept appeared from the idea to apply the constant-velocity accelerating section of finite length, where all cell lengths are identical (gap-to-period ratios might be adapted to rf needs along each cavity finally). The features of the longitudinal motion in constant-β structures have already been described, for example, in [4], especially for the case of small phase variations. The constant periodic length along each cavity must be chosen correspondingly to the average particle velocity expected. The particle motion can be approximately analyzed in the field of the main spatial harmonic:

$$E_z(z,t) = E_m \cos\left(\frac{\pi}{D} z\right) \cdot \cos(\omega t), \tag{1}$$

where E_m is the standing wave amplitude, D is the π-mode structure period, and ω is the angular rf frequency. This standing wave harmonic may be represented as a superposition of the forward and backward traveling waves with amplitudes $E_0 = E_m/2$:

$$E_z(z,t) = E_0\left[\cos\left(\frac{2\pi z}{\beta_S \lambda} - \omega t\right) + \cos\left(\frac{2\pi z}{\beta_S \lambda} + \omega t\right)\right], \tag{2}$$

where $\beta_S = 2D/\lambda$ is the synchronous phase velocity at the

section, λ is the rf wavelength, and $\omega = 2\pi c/\lambda$. Considering the particle velocity close to the phase velocity of the forward wave, we can neglect the averaged oscillating action of backward harmonic. At the same time, the sum of missing kinetic energy and potential energy of a nonsynchronous particle in the field of the forward accelerating harmonic against the synchronous particle must be an invariant:

$$\frac{m(v - v_S)^2}{2} + eq\int_0^{\Delta z} E_z(z)dz = \text{const}, \tag{3}$$

where eq and m denote the charge and the relativistic mass of the ion; v and v_S are nonsynchronous and synchronous velocities, respectively. A parametric equation of the particle trajectory at the phase-velocity plane may be derived from Eq. (3) as follows:

$$(\beta - \beta_S)^2 + \frac{\beta_S \lambda eqE_0}{\pi mc^2} \cdot [\sin(\psi) - \sin(\psi_m)] = 0, \tag{4}$$

where

$$\psi = -\frac{2\pi}{\beta_S \lambda} \cdot \Delta z \tag{5}$$

is the current phase of the particle in the field of accelerating harmonic, Δz is the particle distance to the crest of the wave, and c is the speed of light; ψ_m is the maximum phase, reached by the particle when its velocity exactly equals to the phase velocity of the structure. Note that the phase direction is traditionally opposite to the direction of particle motion. Figure 2 illustrates the evolution of the particle bunch center in the field of an equivalent traveling wave in the phase-velocity plane. Axial distance $\Delta z(z)$ (top) and rf phase $\psi(z)$ (bottom) with respect to the crest

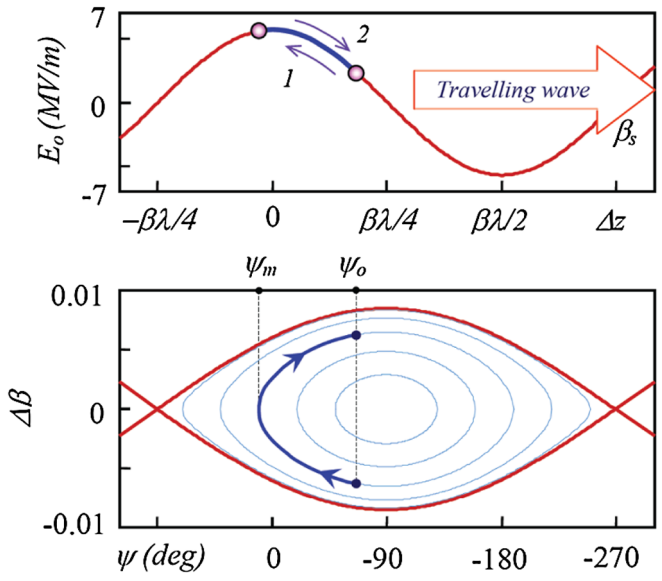

FIG. 2. (Color) Longitudinal motion of an accelerated bunch in the constant-β section against a synchronous particle at $-90°$.

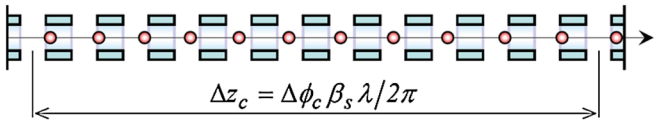

FIG. 3. (Color) Bunch positions at maximum accelerating field in the equidistant section.

of the wave are plotted as abcissas. As this figure shows, the particle bunch enters the section at negative phase, crossing the gap centers at the rising electric field. Since the particle velocity is initially slower than the direct traveling wave, the bunch center slides to the crest of the accelerating field, reaching maximum phase at the middle of the section. Then the accelerated particles become faster and the bunch is moving back to negative phases. As a result, this kind of longitudinal motion locates the bunching and transversally defocusing gaps close to the neighboring lenses, leaving the middle part between lenses for main acceleration close to the crest of the wave. An adequate relation between the total gap number per section and the phase velocity has to be selected for each cavity (see below). In general, the rf phase distribution along each section looks similar to the KONUS beam dynamics, but only constant-β sections are used in this case, while KONUS applies a phase shift after the rebunching section. Figure 3 illustrates the positions of the bunch while passing the crests of the wave along the equidistant section. One can see that the bunch is shifted ahead at the entrance, approaching the gap center in the middle because of velocity lack, and finally it goes ahead again due to the gained acceleration. The same figure defines $\Delta\phi_c$ as an integrated rf phase angle during particle passage from the center of the first gap to the center of the last gap.

In practice, one of the most important questions for this structure is how long may be the equidistant section as a function of the particle energy, accelerating rate, and the range of the phase swing. Unlike particle phase in the accelerating harmonic ψ, introduce the current rf phase as $\phi = \omega t$. Taking into account Eq. (5), the particle velocity deviation from the synchronous value may be expressed by the derivation of these phases:

$$(\beta - \beta_S)/\beta_S = d\psi/d\phi. \tag{6}$$

Substituting Eq. (6) to Eq. (4), total rf phase angle gained between the first and the last gap of the cavity can be found as

$$\Delta\phi_c = -2\sqrt{\frac{\pi mc^2\beta_S}{eq \cdot E_0\lambda}} \cdot \int_{\psi_0}^{\psi_m} \frac{d\psi}{\sqrt{\sin(\psi) - \sin(\psi_m)}}, \tag{7}$$

where ψ_0 is the rf phase of the bunch center when crossing the first and the last gap centers. The exact value of this integral can be calculated only numerically, but may be approximated as follows:

$$\Delta\phi_c \approx 4\sqrt{\frac{\pi mc^2\beta_S}{eq\cdot E_0\lambda}\cdot\left(\sin(\psi_m)-\psi_0-\frac{1}{32}\psi_0^3\right)}. \quad (8)$$

The relative deviation does not exceed 2% if the phase limits are within the ranges $-90° < \psi_0 < 0°$ and $-5° < \psi_m < 15°$. Then the approximate number of accelerating gaps in π-mode structures results in

$$N_g = \frac{\Delta\phi_c}{\pi} + 1. \quad (9)$$

These analytic expressions are in good agreement with the results of beam dynamics simulations. In general, different rf phases at the first and last gap centers are also possible. But as concluded from numerous simulations, this asymmetry does not improve beam dynamics, while additional parameters have to be handled in this case. For this reason, only "symmetrically" focusing periods with identical rf phases at entrance and exit of the sections are recommended.

III. LAYOUT OF AN ENERGY VARIABLE 7.5 AMEV LINAC

According to an actual discussion at GSI, a new cw heavy ion linac should accelerate ions with mass-to-charge ratios $A/q \leq 6$ in the energy range from 1.4 to 7.5 AMeV; the exit energy should be continuously varied from 3.5 AMeV to the maximum value. The upgraded HLI linac [10] is expected to serve as an injector for this machine. While this layout considers a specified case, the concept can be used for similar actual projects as well.

Beam dynamics has been simulated with the LORASR code [11]. A particle array calculated at the output of the existing IH—HLI has been used as an input for these simulations. Since the expected current of highly stripped ions will not exceed 1 mA, space charge effects were supposed to be negligible in designing, but the final result has been checked for 1 mA.

A preliminary calculated layout of the linac behind of 1.4 AMeV is shown at Fig. 4. The room temperature quadrupole triplet at the entrance provides beam transport along a diagnostic box as well as through a rebuncher and along the cold-warm junction into the cryostat. At the same time, it allows one to make the input beam axially symmetric for solenoid focusing along the superconducting linac. The first part of the linac up to the energy of 3.5 AMeV includes three constant cell superconducting cavities with 15, 17, and 19 cells, respectively, and three superconducting solenoids; all parameters of this part are fixed during operation.

As Fig. 5 shows, minimum rf phases of the bunch center at these sections are $-45°$, $-55°$, and $-55°$, respectively, being realized at the first and last cells of each section while the maximum acceleration occurs in the middle. Note that the average phase values for the first three sections are as large as $-19°$, $-22°$, and $-28°$, which is

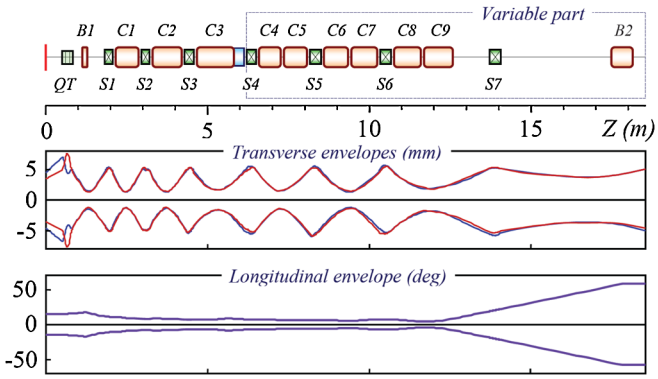

FIG. 4. (Color) Calculated layout of the superconducting heavy ion linac and bunch envelopes; QT = quadrupoletriplet, S_i = solenoid, C_i = cavity, B_i = buncher.

smaller than the typical value of $-30°$, used for traditional structures, but the longitudinal bunch stability is maintained due to the additional alternating effect. Moreover, periodic overbunching at the ends of the sections fits well to this structure with its long focusing periods and separated lenses. Besides the focusing solenoid, a 300 mm drift space at the end of the "fixed energy" part of the linac is reserved for intermediate beam diagnostics.

The variable linac section comprises three focusing periods, each including two 10-gap, constant cell cavities. In principle, beam dynamics would allow long single accelerating sections with 20 gaps and more between solenoids, but two separated superconducting cavities at each focusing period have been decided for the reasons of cavity production and stability. In order to keep the efficient phase profile used at the initial part of the linac, the bunch center starts from the negative phase, namely, $-50°$ at the beginning of the first section and moves to zero phase as Fig. 5 shows. Along the second cavity of each section, the bunch center slides back to the negative phase, coming then to the next solenoid. The only exception is the last section, where the bunch moves from zero to the positive phase direction in order to give the additional debunching energy spread to the particles, reducing the drift space. After a 5 m long drift, when the bunch becomes as long as

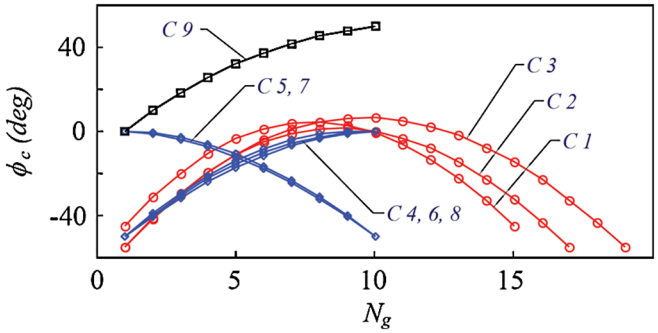

FIG. 5. (Color) The rf phases of the bunch center at the middles of all accelerating gaps along cavities $C1$–$C9$.

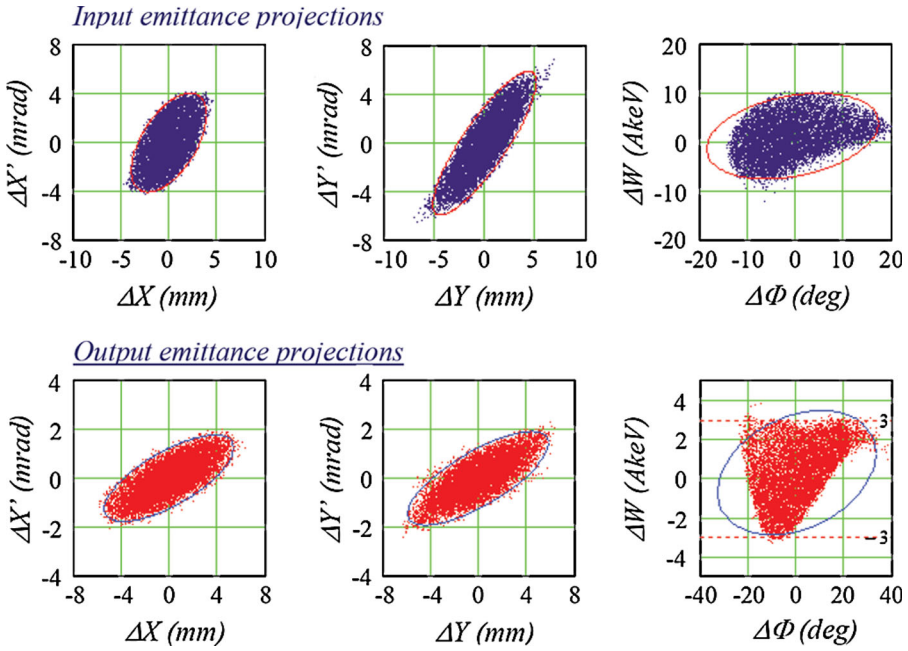

FIG. 6. (Color) Emittance projections at the input and at the output of the superconducting linac for 1 mA beam current.

120° in terms of 216 MHz frequency, the final 108 MHz buncher minimizes the energy spread to the desired value of ±3 AkeV.

The transverse and longitudinal 98% envelopes are presented by Fig. 4. One can see that the beam is close to the axial symmetry and the transverse size does not grow in practice during acceleration. As will be shown below, solenoids of different length are used to keep the beam radius. The longitudinal envelope is slightly reduced along the linac until the beam is debunched at the exit. Figure 6 shows the input and output emittance plots. The energy spread at the linac exit does not exceed the design value of ±3 AkeV.

Figure 7 shows how the rms emittance is increasing along the linac. The average transverse emittance growth does not exceed 5%, while the longitudinal value is around 7% in front of the final rebuncher. The accelerating channel aperture is compared to the transverse beam envelope at Fig. 8; one can deduce a filling factor below 1/3 along the superconducting part.

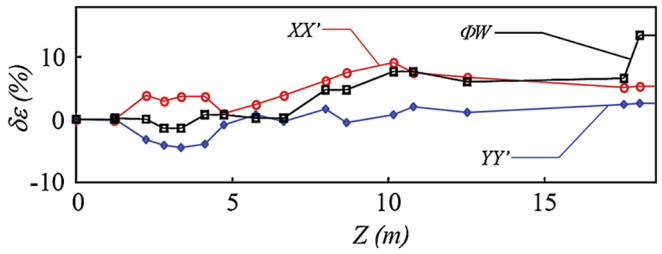

FIG. 7. (Color) The rms emittance growth along the linac for zero beam current.

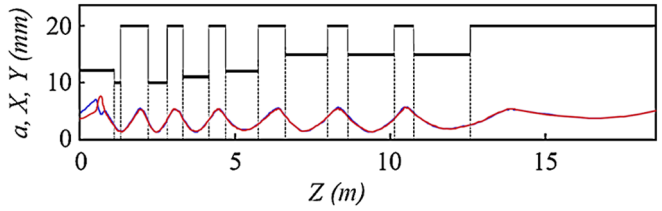

FIG. 8. (Color) Accelerating channel aperture compared to the transverse beam envelope.

IV. ENERGY VARIATION

The rough energy variation is provided by just switching the sections off one after another, starting from the end of the linac as it is practiced successfully with GSI-Unilac. Solenoid gradients should be corrected (reduced) in this case to keep the transverse beam envelope. According to the beam requirements, the energy spread should not exceed ±3 AkeV over the whole range of energy variation. In order to fulfill this condition, the last section should never be completely switched off, but has to operate as an additional debuncher with the bunch center rf phase of +90°. The rf voltage applied to this section has to be properly chosen dependently on the number of operating cavities, keeping the bunch length at the final buncher in the range of 90°–120°. Beam dynamics for all these cases have been simulated by using the LORASR code. Calculations show that the final 10-gap equidistant section efficiently works as a debuncher even for the minimum energy of 3.5 AMeV. The desired result has been achieved

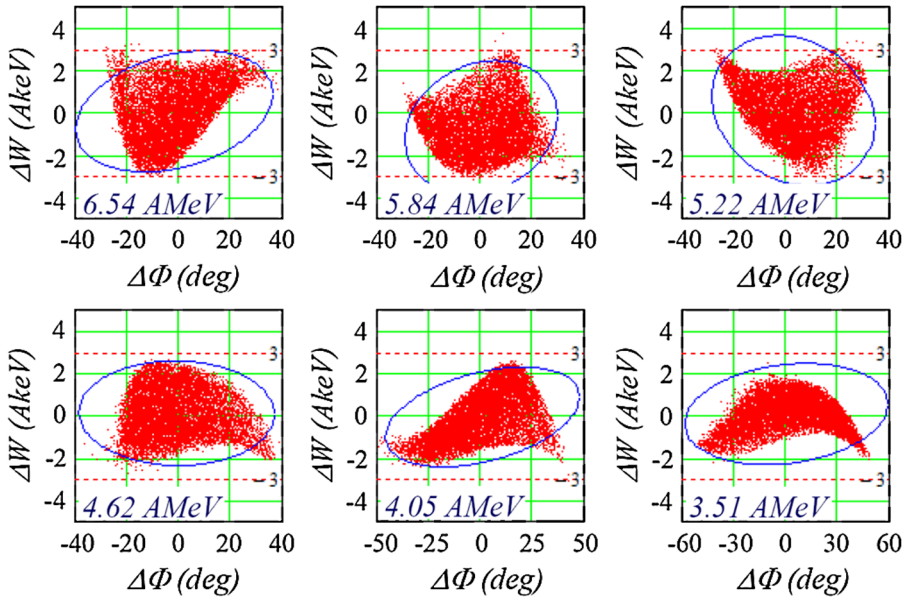

FIG. 9. (Color) Longitudinal emittance plots at the linac exit for different final energies.

by matched rf voltages of the last ninth section, which were always lower than the nominal value for full energy operation. Figure 9 shows the output longitudinal emittance, calculated for different final energies. One can see that the energy spread is kept within the predefined range of ± 3 AkeV.

A simple and convincing way to realize the smooth energy variation is to change the rf voltage applied to the last operating section. As an example, Fig. 10 shows how the exit energy of the seventh section depends on the applied voltage, while Fig. 11 shows the phase profiles of the bunch center for different applied voltages. One can see that the voltage-energy dependence is not exactly linear, but allows easy energy variation.

Another way of a smooth energy variation may be accomplished by varying the rf phase of the amplifier only, at nominal rf level operation. As Fig. 12 shows, if the phase of the bunch center at the first gap of the seventh section is changed from 0° to −90°, the energy gain is reduced to zero, with a further phase decrease particles might be even decelerated. This way of energy variation may be useful if the cavity does not work stably at low voltage levels because, for example, of multipacting. So far, there is no evidence of dangerous multipacting levels at CH cavities.

The obtained results show that an EQUUS section behaves within some parameter range limits similar to the equivalent single gap cavity: the energy gain depends on the applied rf voltage and on the rf phase. Depending on the phase of the bunch center averaged over the gap sequence,

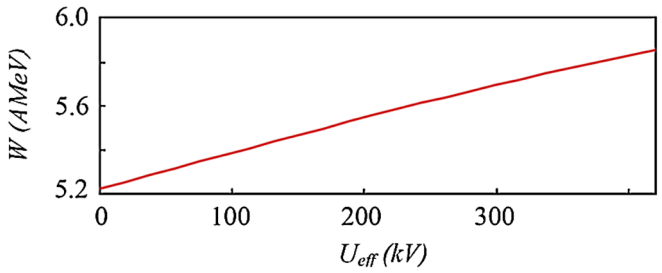

FIG. 10. (Color) Exit energy against applied rf gap voltage for the seventh section.

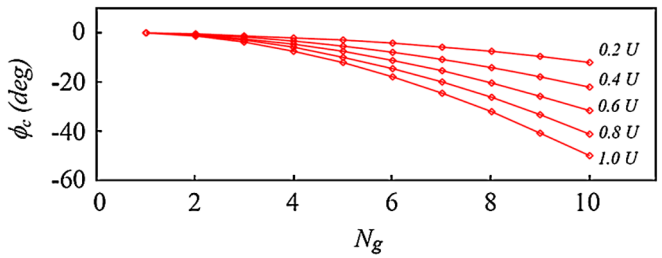

FIG. 11. (Color) Phase profiles of the bunch center for different voltages applied to the seventh section.

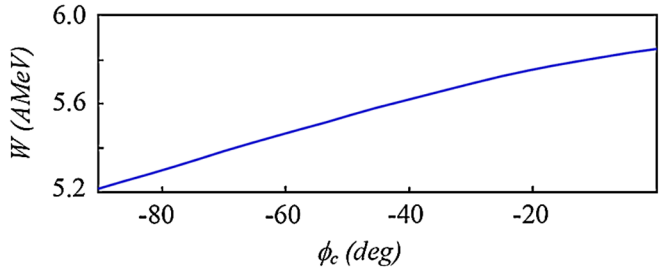

FIG. 12. (Color) Exit energy against initial phase of the bunch center for the seventh section.

this section may work as a buncher or debuncher. The efficiency of such a cavity is determined by the range of the phase swing, which depends on the cavity length and on the particle velocity.

V. PARAMETERS OF THE CALCULATED LINAC LAYOUT

The main parameters calculated for a 7.3 AMeV superconducting linac with energy variation are given by Table I. The second harmonic frequency of the existing HLI linac—216.816 MHz—is chosen for the whole superconducting part of the new linac with the exception of the final room temperature buncher, where the original frequency of 108.408 MHz is used. Even the third harmonic of 324.224 MHz has been initially tested for the superconducting part [12], but the factor 3 in frequency increase was too big, creating considerable emittance growth. Moreover, the cell lengths are too small at the low energy end in this case. Note that the input emittance values are predefined by the existing HLI. The parameters of the individual accelerating cavities are presented by Table II. The largest cavity is as long as 1054 mm, containing 19 accelerating gaps. Even longer superconducting units would cause additional problems in mechanical design and fabrication. This has been learned from the 1 m long, 19-cell prototype cavity. Also with respect to microphonics, Lorentz force detuning, and mode separation, it is wise to limit the cavity length to around 1 m [13]. That is why each focusing period above 3.51 AMeV consists of two separated cavities. In spite of the stable beam diameter calculated along the linac, the aperture of every next cavity is increased by 2 mm in this preliminary design, maintaining the safety margins for possible beam mismatch.

TABLE I. General parameters of superconducting energy variable heavy ion linac.

Charge-to-mass ratio		1/6
Operating frequency	MHz	216.816
Beam current	mA	1
Injection energy	AMeV	1.39
Input transverse emittance, (normalized)	mm mrad	0.8π
Input longitudinal emittance, (normalized)	AkeV ns	1.9
Output energy	AMeV	3.51–7.30
Output energy spread	AkeV	± 3
Transverse rms emittance growth	%	5
Longitudinal rms emittance growth	%	6
Total length with debunching growth	m	18.5
Length of accelerating part	m	12.7
Number of SC accelerating cavities		9
Number of SC solenoids		7

The parameter named "phase factor" characterizes the accelerating efficiency with respect to the phase sliding along the section. It has been specified as

$$PF = \frac{1}{N_g} \sum_{i=1}^{N_g} \cos(\phi_{ci}), \tag{10}$$

where ϕ_{ci} is the phase of the bunch center in the ith accelerating gap. As Table II shows, phase factors are higher than 0.9 for all sections except the last one, which operates as a debuncher.

Table III shows the parameters of the superconducting solenoids used for beam focusing. The induction values do not exceed 10 T, the aperture diameter is assumed as large as 50 mm. Different solenoid lengths of 250, 300, and 350 mm allow one to keep the beam diameter along the linac without a significant increase of field levels.

The main parameters of the rebunching cavities are given at Table IV. The front-end, two-gap buncher needs an effective gap voltage of 145 kV, while a gap voltage of 213 kV has to be applied to the 108 MHz four-gap buncher at the exit. Table V shows the parameters of the input room temperature triplet. The effective pole lengths are given in the table, leading to the shorter interpole distances compared to the realistic geometry. Furthermore, the only special feature of this device is that the gradients in all lenses are different in order to form an axisymmetric beam at the input of the solenoid-focused superconducting part of the linac.

TABLE II. Parameters of the superconducting multigap accelerating cavities.

Parameter	Unit	C1	C2	C3	C4	C5	C6	C7	C8	C9
Gap number		15	17	19	10	10	10	10	10	10
Total length	mm	613	811	1054	639	639	726	726	813	862
Cell length	mm	40.8	47.7	55.5	63.9	63.9	72.6	72.6	81.3	86.2
Synchronous veloctiy		0.059	0.069	0.080	0.092	0.092	0.105	0.105	0.118	0.125
Aperture diameter	mm	20	22	24	30	30	30	30	30	30
Effective gap voltage	kV	225	274	317	356	362	408	411	459	538
Voltage gain	MV	3.13	4.14	5.42	3.27	3.30	3.73	3.73	4.18	4.43
Phase Factor		0.93	0.89	0.90	0.92	0.91	0.92	0.91	0.91	0.82
Accelerating rate	MV/m	5.1	5.1	5.1	5.1	5.1	5.1	5.1	5.1	5.1

TABLE III. Parameters of the superconducting solenoids.

Parameter	Unit	S1	S2	S3	S4	S5	S6	S7
Effective length	mm	250	250	300	300	350	350	350
Magnetic induction	T	8.15	9.5	9.1	9.15	9.6	10.0	6.5
Aperture diameter	mm	40	40	40	40	40	40	40

TABLE IV. Parameters of bunching cavities.

Parameter	Unit	B1	B2
Operating frequency	MHz	216.816	108.408
Gap number		2	4
Total length	mm	75.4	687.2
Period length	mm	37.7	171.8
Aperture diameter	mm	20	50
Effective gap voltage	keV	145	213

TABLE V. Parameters of the front room temperature triplet.

Parameter	Unit	Q1	Q2	Q3
Effective pole length	mm	77	138	77
Gradient	T/m	61	57	51
Interpole distance	mm	22	22	22
Aperture diameter	mm	24	24	24

VI. CH CAVITY DEVELOPMENT

The CH cavity is operated in the H_{210} mode and it belongs to the family of H-mode cavities like the IH drift tube cavity and the four-vane radio frequency quadrupole.

Because of the mechanical rigidity of the CH cavity, room temperature as well as superconducting versions can be realized. For higher duty cycles or even cw operation, superconducting solutions become more favorable or even the only choice because of a lower plug power consumption and higher achievable gradients. In many cases the rf linac efficiency and compactness can be increased significantly by the use of multicell cavities.

The superconducting CH-prototype cavity ($f = 360$ MHz, $\beta = 0.1$, 19 cells) has been developed and tested successfully in Frankfurt. After a second chemical surface preparation gradients of 7 MV/m corresponding to an effective voltage of 5.6 MV have been achieved (Fig. 13). At present a superconducting 325.224 MHz CH cavity is under development.

This cavity can be considered as a second prototype for the proposed accelerator scheme. It will consist of seven accelerating cells. The frequency is three times the frequency of the Unilac heavy ion accelerator at GSI. The design beta is 0.158 which corresponds to the Unilac output energy of 11.4 AMeV. This cavity will be equipped with all necessary auxiliaries like power couplers, tuning systems, and helium vessel.

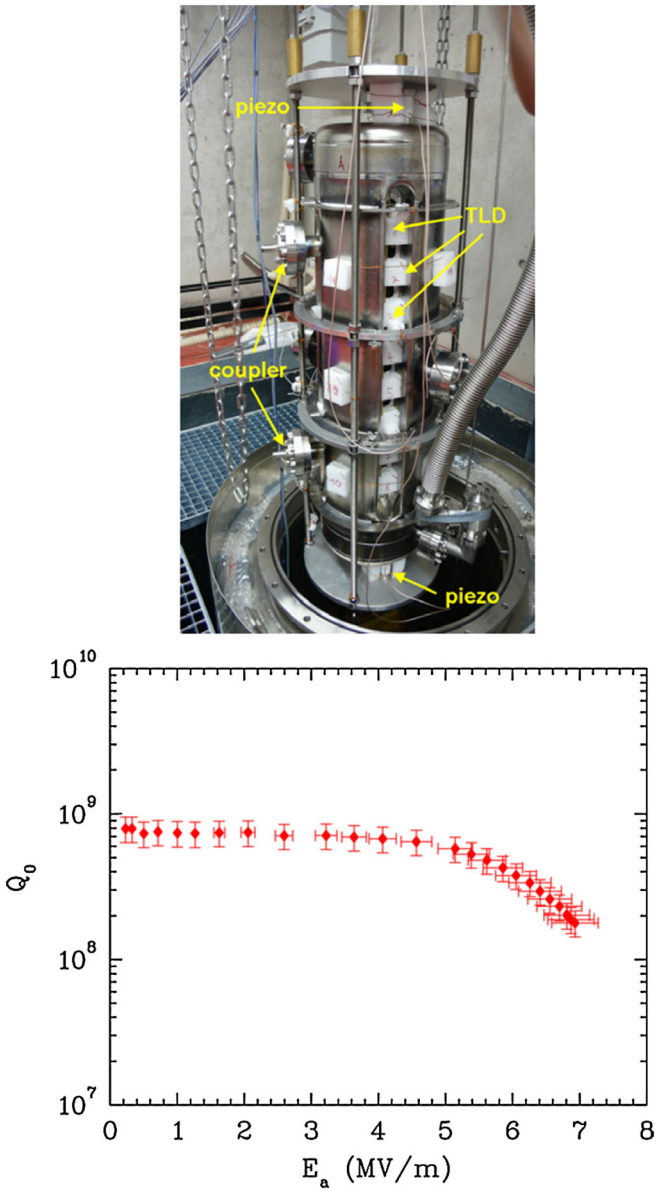

FIG. 13. (Color) Experimental setup for testing the superconducting CH-prototype cavity in the cryogenic laboratory in Frankfurt; piezo = fast tuning device, TLD = thermo luminescence dosimeter (top). Measured Q value as a function of the accelerating gradient. The achieved gradient of 7 MV/m corresponds to an effective voltage gain of 5.6 MV (bottom).

It is planned to test this new cavity with beam to demonstrate its capabilities under a realistic accelerator environment and at full rf power.

To fulfill the requirements for high power operation, the geometry of the new superconducting CH cavity has been optimized (Fig. 14). The stem orientation has been changed to accommodate sufficiently large power couplers into the girder. The stems of the end cells are inclined. This increases the inductance in the end cells and increases the electric on-axis field without long end drift tubes which have been used before. This has great advantages for the

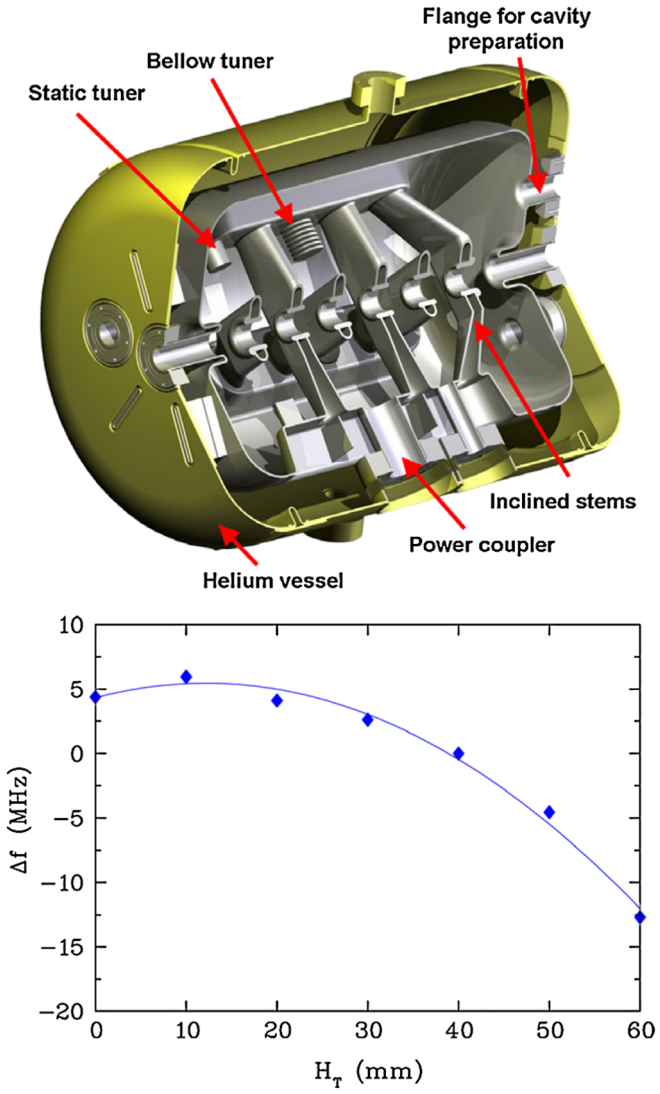

FIG. 14. (Color) Geometry of the superconducting seven-cell, $f = 325.224$ MHz, $\beta = 0.158$ CH cavity which is at present under construction (top). Tuning range as a function of the tuner height (bottom).

beam dynamics of high intensity linacs. The drawback of inclined stems is an increased magnetic peak field of 13 mT/(MV/m). On the other hand, typical gradients of 5 MV/m lead to still modest values of 65 mT only. To reach the design frequency it is planned to use six cylindrical tuners with $r \approx 15$ mm welded into the girders. During the fabrication the frequency is controlled and will be adapted accordingly. This procedure has been tested successfully at the first prototype cavity. Additionally, two bellow tuners with $r \approx 25$ mm are foreseen. One tuner will act as a slow tuner to compensate temperature and pressure effects. The other tuner will be driven by a piezo to control fast frequency changes. Figure 14 shows the simulated frequency shift as a function of the tuner height above the girder H_T using all eight

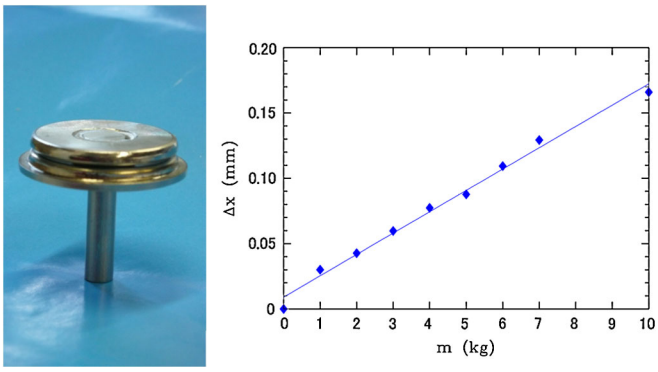

FIG. 15. (Color) Bellow tuner from niobium with 1.5 segments for mechanical tests (left) and results from measurement at room temperature (right).

tuners simultaneously. A first prototype of the bellow tuner is shown by Fig. 15.

The experience with the first prototype cavity showed that a good surface preparation is essential for the performance of the cavity. Therefore four additional flanges, two located at each end plate, are foreseen now to improve the thoroughness of the surface preparation (buffered chemical polishing, high pressure rinsing).

The proposed cw linac for super heavy element (SHE) production and nuclear chemistry in general will consist of nine superconducting CH cavities operated at 216.816 MHz. Figure 16 shows the designed integration of that linac at GSI and the beam inflection just behind Unilac, so that the beams of the new linac can be sent to the SHE detector SHIP as well as to all other experiments (for example, exotic ions from the electron-cyclotron-resonance source or low current test beams for the future FAIR complex).

Figure 17 shows as an example the design of the 217 MHz cavity C5 as characterized in Table II.

VII. CONCLUSIONS

1. An equidistant multigap accelerating structure EQUUS has been found and in this paper investigated. The phase sliding of the bunch, unavoidable in the constant-period section, has been used to form a special type of the longitudinal motion, which fits very well to the efficient, low-capacitive H-type structures with separated focusing lenses.

2. The cell periodicity of the accelerating cavity gives the following technical advantages: (i) higher calculation accuracy; (ii) easier manufacturing compared to the cavity with different sizes of the tubes and gaps; (iii) easier tuning procedure due to permanent capacitive loading; (iv) easier energy variation. All these advantages become especially important for superconducting structures.

3. A preliminary design of the cw superconducting linac dedicated for a competitive SHE research program at GSI has been worked out. As the beam dynamics simulations

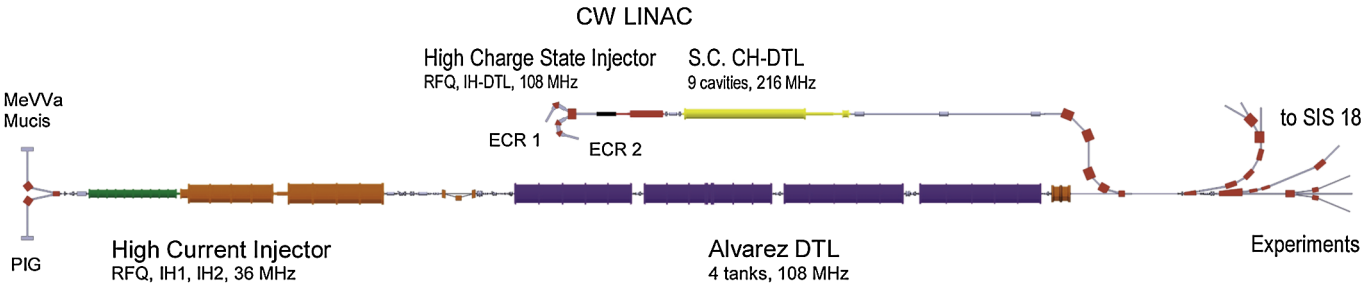

FIG. 16. (Color) Schematic overview of the GSI Unilac and integration of the cw linac comprising the 1.4 AMeV high charge state injector and the new superconducting CH section. The beam inflection into the main beam line allows beam transport to all experimental areas.

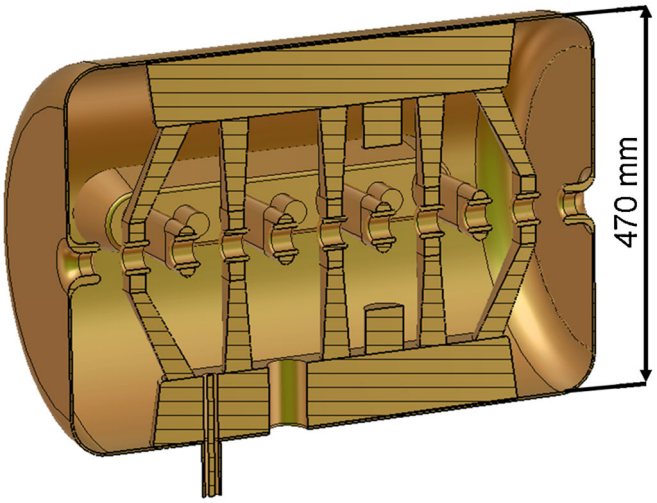

FIG. 17. (Color) Layout of the 217 MHz cavity C5, calculated with CST MICROWAVE STUDIO [14].

show, all design requirements are fulfilled by EQUUS, including the small energy spread of 3 AkeV over the whole energy range from 3.5 to 7.3 AMeV.

ACKNOWLEDGMENTS

This work has been supported by Gesellschaft für Schwerionenforschung (GSI), BMBF Contract No. 06F134I, EU-FP6 (CARE, Contract No. RII3-CT-2003-506395) and EU Contract No. EFDA/99-507ERB5005 CT990061 (IFMIF), and by LOEWE-HIC for FAIR. The authors would like to thank the company ACCEL for the excellent work on technical drawings as well as in the fabrication of the prototype cavity. In addition, the authors would like to thank the technical staff of the IAP in Frankfurt, especially D. Bänsch, I. Müller, and S. Reploeg. They would also like to thank F. Dziuba and R. Tiede for their help in preparing the manuscript.

[1] U. Ratzinger *et al.*, Nucl. Instrum. Methods Phys. Res., Sect. A **415**, 229 (1998).
[2] H. Podlech *et al.*, Phys. Rev. ST Accel. Beams **10**, 080101 (2007).
[3] U. Ratzinger, in Proceedings of the 1991 Particle Accelerator Conference, San Francisco, 1991, pp. 567–571.
[4] T. P. Wangler, *RF Linear Accelerators* (Wiley, New York, 2008).
[5] L. M. Bollinger *et al.*, in Proceedings of the Linear Accelerator Conference, Chalk River, Canada, 1976, pp. 95–101.
[6] R. Delayen *et al.*, IEEE Trans. Nucl. Sci. **32**, 3590 (1985).
[7] I. Ben-Zvi *et al.*, Nucl. Instrum. Methods **212**, 73 (1983).
[8] K. W. Shepard *et al.*, in Proceedings 1998 Linear Accelerator Conference, Argonne, IL, 1998, pp. 956–958.
[9] J. Broere *et al.*, in Proceedings 1998 Linear Accelerator Conference, Argonne, IL, USA, 1998, pp. 771–773.
[10] P. Gerhard *et al.*, in *Proceedings of the 11th European Particle Accelerator Conference, Genoa, 2008* (EPS-AG, Genoa, Italy, 2008), p. 3416.
[11] R. Tiede *et al.*, in Proceedings of the XXII International Linear Accelerator Conference, Lübeck, Germany, 2004, p. 60.
[12] R. Eichhorn, in *Proceedings of the 19th Particle Accelerator Conference, Chicago, Illinois, 2001* (IEEE, Piscataway, NJ, 2001), pp. 495–499.
[13] A. Bechtold *et al.*, in Proceedings of the 2007 Superconducting RF Workshop, Bejing, China, p. 618
[14] http://www.cst.com/.